BIOCHEMISTRY
including biophysical chemistry & molecular biology
Article

Biochemistry **2009,** *48,* 7009–7018 7009
DOI: 10.1021/bi900515d

Understanding How Diverse β-Mannanases Recognize Heterogeneous Substrates†

Louise E. Tailford,[‡,@] Valerie M.-A. Ducros,[§] James E. Flint,[‡] Shirley M. Roberts,[§] Carl Morland,[‡] David L. Zechel,[∥] Nicola Smith,[‡] Mads E. Bjørnvad,[⊥] Torben V. Borchert,[⊥] Keith S. Wilson,[§] Gideon J. Davies,[*,§] and Harry J. Gilbert[*,‡,#]

[‡]*Institute for Cell and Molecular Biosciences, Newcastle University, The Medical School, Newcastle upon Tyne NE2 4HH, U.K.,* [§]*York Structural Biology Laboratory, Department of Chemistry, University of York, Heslington, York YO10 5YW, U.K.,* [∥]*Department of Biochemistry, Queen's University, Kingston K7L 3N6, Ontario, Canada, and* [⊥]*Novozymes A/S, Brudelysvej 26, 2880 Bagsvaerd, Denmark.* [@]*Current address: Institute of Food Research, Colney Lane, Norwich NR4 7UA, U.K.* [#]*Current address: Complex Carbohydrate Research Center, University of Georgia, 315 Riverbend Rd., Athens, GA 30602-4712*

Received March 25, 2009; Revised Manuscript Received May 12, 2009

ABSTRACT: The mechanism by which polysaccharide-hydrolyzing enzymes manifest specificity toward heterogeneous substrates, in which the sequence of sugars is variable, is unclear. An excellent example of such heterogeneity is provided by the plant structural polysaccharide glucomannan, which comprises a backbone of β-1,4-linked glucose and mannose units. β-Mannanases, located in glycoside hydrolase (GH) families 5 and 26, hydrolyze glucomannan by cleaving the glycosidic bond of mannosides at the −1 subsite. The mechanism by which these enzymes select for glucose or mannose at distal subsites, which is critical to defining their substrate specificity on heterogeneous polymers, is currently unclear. Here we report the biochemical properties and crystal structures of both a GH5 mannanase and a GH26 mannanase and describe the contributions to substrate specificity in these enzymes. The GH5 enzyme, *Ba*Man5A, derived from *Bacillus agaradhaerens*, can accommodate glucose or mannose at both its −2 and +1 subsites, while the GH26 *Bacillus subtilis* mannanase, *Bs*Man26A, displays tight specificity for mannose at its negative binding sites. The crystal structure of *Ba*Man5A reveals that a polar residue at the −2 subsite can make productive contact with the substrate 2-OH group in either its axial (as in mannose) or its equatorial (as in glucose) configuration, while other distal subsites do not exploit the 2-OH group as a specificity determinant. Thus, *Ba*Man5A is able to hydrolyze glucomannan in which the sequence of glucose and mannose is highly variable. The crystal structure of *Bs*Man26A in light of previous studies on the *Cellvibrio japonicus* GH26 mannanases *Cj*Man26A and *Cj*Man26C reveals that the tighter mannose recognition at the −2 subsite is mediated by polar interactions with the axial 2-OH group of a $^4C_1$ ground state mannoside. Mutagenesis studies showed that variants of *Cj*Man26A, from which these polar residues had been removed, do not distinguish between Man and Glc at the −2 subsite, while one of these residues, Arg 361, confers the elevated activity displayed by the enzyme against mannooligosaccharides. The biological rationale for the variable recognition of Man- and Glc-configured sugars by β-mannanases is discussed.

The plant cell wall comprises an elaborate array of chemically distinct interlocking polysaccharides (*1*). The microbial degradation of the plant cell wall not only is important in maintaining terrestrial and marine life but also is of growing industrial interest, particularly in the bioenergy and bioprocessing sectors (*1*). Indeed, the rate of plant cell wall hydrolysis is considered by some to be the rate-limiting step in the production of so-called "second-generation" lignocellulose-derived liquid fuels such as ethanol (*1*). The plant cell wall is degraded by an array of glycoside hydrolases and carbohydrate esterases, which have been grouped into sequence-based families (*2*). Families in which the overall fold, catalytic mechanism, and catalytic apparatus are conserved have been further grouped into clans (*3*). Saprophytic microorganisms that use the plant cell wall as a significant nutrient synthesize extensive repertoires of degradative enzymes reflecting the chemical complexity of the composite substrate (*4*, *5*). Indeed, the majority of these organisms express ∼100 extracellular plant cell wall hydrolases, although some specialized pectin-degrading bacteria produce more than 200 enzymes that target plant polysaccharides (*6*). One of the intriguing features of plant cell wall-degrading enzyme systems is the presence of large numbers of closely related enzymes, which likely reflect an evolutionary pressure to accommodate the subtle differences in the structure of the cell wall polysaccharides that occur both

†This work was funded by the Biotechnology and Biological Sciences Research Council (BBSRC) of the United Kingdom. N.S. thanks the European Commission for provision of a "Marie-Curie" fellowship. G.J.D. is a Royal Society-Wolfson Research Merit Award holder.

*To whom correspondence should be addressed. H.J.G.: e-mail, h.j.gilbert@ncl.ac.uk; telephone, +1-706-585-0655; fax, +1-706-542-4412. G.J.D.: e-mail, davies@ysbl.york.ac.uk; telephone, +44-(0)1904-328260; fax, +44-(0)1904-328266.

Published on Web 05/14/2009

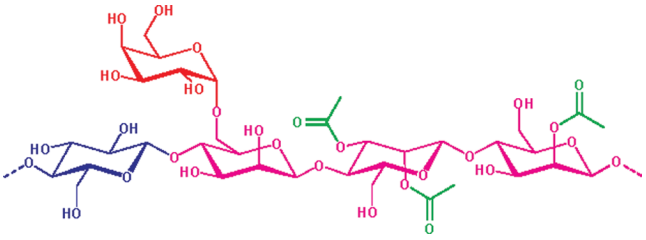

FIGURE 1: Example of the diversity displayed by mannans. The mannose backbone (magenta) of mannans may include glucose (blue) in glucomannans and may also be appended with 6-*O* α-galactosides (red) in galactomannans and glucogalactomannans. Acetate groups (green) may also be found on the O2 and O3 hydroxyls.

between species and within one organism in a way that reflects tissue differentiation. Understanding the biochemical significance of, and the underlying structural basis for, the large number of "isoenzymes" in plant cell wall-degrading systems represents a significant challenge.

Some of the most diverse plant cell wall polysaccharides are those containing β-1,4-linked mannosides (Figure 1). These molecules can be homopolymers of β-1,4-linked mannose (Man) resides, termed mannans, or galactomannans in which the mannan backbone is additionally decorated with α-1,6-galactosyl moieties. Glucomannans, in contrast, have a heterogeneous backbone of β-1,4-linked mannosyl and glucosyl (Glc) sugars that may be augmented, at Man, with α-1,6-galactoside (Gal) side chains (decorated glucomannans define a galactoglucomannan). Furthermore, all forms of mannan and glucomannan may also be acetylated at O2 or O3 (*7*, *8*). The mannosidic bonds in mannans and glucomannans are hydrolyzed by β-mannanases (*9*) found in glycoside hydrolase families (GHs) 5 and 26 (*10*), which are members of clan GH-A (*3*). Both enzyme families hydrolyze the glycosidic bond by a double displacement or "retaining" mechanism (*11*) (recently reviewed in ref (*12*)). Recent studies suggest that the specificity of retaining β-mannanases and β-mannosidases at the critical −1 subsite [glycoside hydrolases cleave the glycosidic bond between the sugars located at the −1 and +1 subsites (nomenclature in ref (*13*))] is through recognition of the $B_{2,5}$ conformation, adopted at or near the transition state, in which the key specificity determinant is the pseudoaxial O3 atom (*14*−*17*). Although there is theoretical support for such itineraries (*18*), there is a single report which maintains that retaining β-mannanases are unlikely to favor a boat conformation at the transition state (*19*).

Selected saprophytic microorganisms that can rapidly hydrolyze mannans express a range of GH5 and GH26 mannanases (*4*, *10*). It is possible that the biological rationale for these mannanase isoenzymes reflects the lack of a defined sequence of Man and Glc in the glucomannan backbone. Indeed, recent studies have shown that *Cellvibrio japonicus* expresses a GH5 mannanase, *Cj*Man5A, which can accommodate Glc at subsites flanking the critical −1 subsite, while two GH26 enzymes from the same bacterium display tight specificity for Man at its negative subsites (*10*, *14*). The extent to which mannanases can accommodate Glc as well as Man in distal sugar binding sites and the mechanism by which these enzymes display relaxed or tight substrate specificities are currently unclear. Here we report the biochemical properties of a GH5 and GH26 mannanase, and the use of structural information to probe the mechanism of sugar selection within the substrate binding cleft. The data show that GH5 mannanases generally display relaxed specificity for Glc or Man at subsites that flank the −1 subsite, either by not selecting O2 as a specificity determinant or by deploying polar residues that can interact with either an axial (as in Man) or equatorial (as in Glc) O2. Mutagenesis studies reveal how relaxed substrate specificity can be engineered into a GH26 mannanase.

MATERIALS AND METHODS

Cloning, Expression, and Purification of GH26 and GH5 Mannanases. The open reading frame encoding mature form of the mannanase *Bs*Man26A was amplified from *Bacillus subtilis* 168 genomic DNA by PCR using forward and reverse primers designed for cloning into the Ek/LIC pET vector (Novagen): 5′-GACGACGACAAGATGCATACTGTGTCGCCTGTGAATCCTAATGC-3′ and 5′-GAGGAGAAGCCCGGTCTCAACGATTGGCGTTAAAGAATCAC-3′, respectively. The resultant product was annealed into Ek/LIC vector pET32a (Novagen) to produce expression construct p*Bs*Man26A containing a C-terminal His_6 tag. *Bs*Man26A (GenBank accession number BAA19712.1) was produced in *Escherichia coli* BL21 DE3 (Novagen) cells, harboring p*Bs*Man26A, cultured in LB broth containing ampicillin (50 μg/mL) at 37 °C. Cells were grown to midexponential phase (A_{600} of 0.6), at which point isopropyl β-D-thiogalactopyranoside was added to a final concentration of 1 mM, and the cultures were incubated for a further 16 h at 16 °C. The cells were harvested by centrifugation, and His_6-tagged recombinant protein was purified from cell-free extracts by immobilized metal ion affinity chromatography using the standard methodology (*20*). Recombinant forms of the two *C. japonicus* mannanases, *Cj*Man26A (GenBank accession number CAA57670.2) and *Cj*Man5A (GenBank accession number ACE84673.1), were expressed in *E. coli* and purified to electrophoretic homogeneity as described by Hogg et al. (*10*). The *Bacillus agaradhaerens* mannanase, *Ba*Man5A (sequence can be found in PDB entry 2whj), was cloned by PCR amplification from *B. agaradhaerans* (strain NCIMB 40482) genomic DNA using the following primers: 5′-CATTCTGCAGCCGCGGCAGCAAGTACAGGCTTTTATGTTGATGG-3′ and 5′-GACGACGTACAAGCGGCCGCGCTATTTCCCTAACATGATGATA TTTTCG-3′, containing SacII and NotI sites (underlined), respectively. The gene was cloned into expression vector pMOL944, which supplied a signal peptide and placed the gene under transcriptional control of the Termamyl-amylase promotor. A *B. subtilis* strain was transformed with the plasmid and incubated in shake flasks using a rich growth medium. After incubation for 5 days at 37 °C, the fermentation broth was flocculated, filtered, and concentrated by ultrafiltration. The mannanase was purified using anion-exchange chromatography on a Q-Sepharose column in 50 mM Tris-HCl buffer (pH 7.5) deploying a NaCl gradient. Finally, proteases were removed using a Bacitracin column followed by size exclusion chromatography using a Superdex 75 column. The electrophoretically pure enzyme has an M_r of 38000 as estimated by SDS−PAGE.

Mutagenesis. Site-directed mutagenesis was conducted using the PCR-based QuikChange site-directed mutagenesis kit (Stratagene) according to the manufacturer's instructions, using pDB1 (encodes *Cj*Man26A) as the template and primer pairs that are listed in Table 1.

Enzyme Assays. Enzyme assays using polysaccharides or mannooligosaccharides were conducted as described by Hogg et al. (*10*). The hydrolysis of polysaccharides, conducted in 50 mM sodium phosphate buffer (pH 7.0) containing 1 mg/mL BSA, was analyzed by the determination of reducing sugar

Table 1: Primers Used To Generate *Cj*Man26A Mutants

name[a]	sequence
E121AF	3′-GCC CCT AAA GCG GCG GGC GAT ATT GTC G-5′
E121AR	3′-CGA CAA TAT CGC CCG CCG CTT TAG GGG C-5′
R361AF	3′-GCT GGT ATG GGC CAA TGC CCC GCA GG-5′
R361AR	3′-CCT GCG GGG CAT TGG CCC ATA CCA GC-5′
H377AF	3′-GCA CCC AGG TTC CCG CGT ATT GGG TGC CTG C-5′
H377AR	3′-GCA GGC ACC CAA TAC GCG GGA ACC TGG GTG C-5′

[a] The name identifies the mutation constructed and whether the sequence corresponds to the sense (F) or antisense (R) strand of the gene.

release. The hydrolysis of mannooligosaccharides, which was conducted in 50 mM sodium phosphate/12 mM citrate buffer (pH 6.5), was assessed by measuring the rate of substrate depletion using HPLC. The concentration of substrate deployed (30 μM) was well below the K_M as there was a linear relationship between substrate concentration and the rate of hydrolysis up to 100 μM. Thus, the rate of hydrolysis of mannooligosaccharides gives a direct readout of k_{cat}/K_M (see refs (*21*) and (*22*)). HPLC was used to determine the rate of release of Glc-Man from glucomannan using a standard of the disaccharide generously provided by B. McCleary (Megazyme International, Bray, Ireland). The hydrolysis of 4-nitrophenyl-β-D-Man_2 ($4NPMan_2$)[1] and 4-nitrophenyl-β-D-Man-Glc [4NPManGlc; synthesis of these aryl glycosides, a kind gift from S. Withers, University of British Columbia (Vancouver, BC), will be described elsewhere], which was conducted in the sodium phosphate buffer described above, was monitored kinetically by the release of 4-nitrophenolate using a molar extinction coefficient of 8750 M^{-1} cm^{-1}, determined from measuring the A_{400} of 4-nitrophenolate at concentrations ranging from 0 to 100 μM.

(i) Crystallization, Data Collection, and X-ray Structure Determination of BaMan5A in Native and Complexed Forms. Crystals of *Ba*Man5A were grown from 1.8 M ammonium sulfate in 0.1 M sodium citrate buffer (pH 6.5). Single crystals were mounted and data collected on the native form of *Ba*Man5A using an "in house" Cu Kα rotating anode generator with a MAR Research image plate as a detector. Data were collected to approximately 1.8 Å resolution from a crystal frozen with 25% (v/v) glycerol as the cryoprotectant. These and subsequent data were processed with DENZO/SCALEPACK (*23*) or MOSFLM [from the CCP4 suite (*24*)] with all subsequent computing using the CCP4 suite, unless otherwise stated. The *Ba*Man5A native crystals were in space group $P6_1$, with the following cell dimensions: $a = b = 112.0$ Å, $c = 47.4$ Å $\alpha = \beta = 90°$, and $\gamma = 120°$. The structure was determined by molecular replacement with AMORE (CCP4 suite version) using the *Thermobifida fusca* GH5 mannanase as a search model with data between 20 and 3.0 Å and an outer radius of Patterson integration of 25 Å. The structure was refined using REFMAC (*25*) with final manual corrections using COOT (*26*).

The Y6S mutant of *Ba*Man5A, obtained serendipitously through PCR-induced error, crystallized in a different form that was more amenable to soaking studies. Crystals grew from a 1.6 M sodium dihydrogen phosphate/potassium dihydrogen phosphate mixture with 0.1 M Hepes/Na buffer (pH 7.5). The ratio of protein (approximately 30 mg/mL) to mother liquor was 1:1 in sitting drops. Crystals were mounted in stabilizing mother liquor with the inclusion of 30% (v/v) ethylene glycol as a cryoprotectant. Data were collected to 1.4 Å at the European Synchrotron Radiation Facility (ESRF) on beamline ID14-4 using an ADSC quantum-4 CCD detector. The space group was $P2_12_12_1$ with a single molecule of the mannanase in the asymmetric unit and the following cell dimensions: $a = 58.3$ Å, $b = 63.7$ Å, $c = 83.6$ Å, and $\alpha = \beta = \gamma = 90°$. The structure was determined and refined as described above, but using the native *Ba*Man5A coordinates as the search model.

(ii) Crystallization, Data Collection, and X-ray Structure Determination of BsMan26A. *Bs*Man26A at 10−20 mg/mL was crystallized, originally from a sample provided by Novozymes A/S, from 35% (v/v) PEG 8K with 0.2 M sodium acetate buffer in 0.1 M Tris-HCl buffer (pH 7−8.0). Data were collected, to 1.7 Å resolution, on beamline ID14-4 of ESRF. Crystals were in space group $P3_1$ with a single molecule of *Bs*Man26 in the asymmetric unit and the following cell dimensions: $a = b = 67.5$ Å, $c = 72.9$ Å, $\alpha = \beta = 90°$, and $\gamma = 120°$. The structure was determined using the CCP4 implementation of MOLREP using the protein coordinates of only the *Cj*Man26A trapped intermediate complex as the search model. During the course of this work, the structure of *Bs*Man26A was also determined by the New York Structural GenomiX Research Consortium (PDB entry 3CBW).

(iii) Crystallization, Data Collection, and X-ray Structure Determination of the CjMan26A Variant E121A/E320A in Complex with Mannotetraose. The *Cj*Man26A variant E121A/E320G at 30 mg/mL was crystallized in 100 mM Tris-HCl buffer (pH 7.5), 26% (v/v) monomethylether PEG 550, and 3 mM $ZnSO_4$. Crystals were frozen using the crystallization buffer supplemented with PEG 550 to 30% (v/v) MME as the cryoprotectant. Data were collected to 1.5 Å resolution, on beamline ID14-4 of ESRF. Crystals were in space group $P4_1$ with one molecule of the enzyme in the asymmetric unit and the following cell dimensions: $a = b = 93.2$ Å, $c = 53.8$ Å, and $\alpha = \beta = \gamma = 90°$. The structure was essentially isomorphous with past *Cj*Man26A structures and so was simply refined using REFMAC, following initial rigid body refinement of the protein atoms of only the *Cj*Man26A trapped intermediate complex (*15*). Details of X-ray data collection and structure refinement for all structures in this paper are listed in Table 2.

RESULTS

Biochemical Properties of GH5 and GH26 Mannanases. To dissect the subsite specificity of mannanases on heterogeneous substrates, the biochemical properties of *Bs*Man26A and *Ba*Man5A, determined here, are compared with those of previously characterized mannanases (*Cj*Man5A and *Cj*Man26A) (Table 3). The activity of *Ba*Man5A against glucomannan and galactomannan was typical of GH5 and GH26 mannanases (*10*, *14*, *21*). By contrast, in these experiments, *Bs*Man26A was 100−1000-fold less active than the *C. japonicus* and *Bacillus* mannanases, against these polysaccharides. The two *Bacillus* mannanases exhibited very low catalytic efficiencies against mannotriose (Man_3), suggesting that the subsites immediately flanking the −1 subsite contribute comparatively little to catalysis. Typical of *endo*-acting glycoside hydrolases, there was a substantial increase (100−1000-fold) in the activity of *Ba*Man5A and *Bs*Man26A

[1] Abbreviations: M_2, mannobiose; M_3, mannotriose; M_4, mannotetraose; $4NPMan_2$, 4-nitrophenyl-β-D-Man_2; 4NPManGlc, 4-nitrophenyl-β-D-Man-Glc; rmsd, root-mean-square deviation; PDB, Protein Data Bank.

Table 2: Crystal, Data, and Refinement Statistics for *Ba*Man5, *Bs*Man26, and *Cj*Man26A Mutants

	*Ba*Man5 native	*Ba*Man5 Man_3	*Bs*Man26	*Cj*Man26A E121A/E320G Man_2
space group	$P6_1$	$P2_12_12_1$	$P3_1$	$P4_1$
Data Quality				
X-ray source	Cu Kα	ESRF ID14-4	ESRF ID14-4	ESRF ID14-1
resolution of data (Å)	20−1.78	20−1.4	20−1.7	30−1.5
resolution of outer shell (Å)	1.84−1.78	1.45−1.4	1.76−1.7	1.55−1.50
R_{merge} (outer shell)	0.050 (0.10)	0.053 (0.20)	0.053 (0.12)	0.038 (0.27)
mean $I/\sigma I$ (outer shell)	42 (6.8)	27 (3.5)	44 (7.1)	53 (5.2)
completeness (outer shell) (%)	94 (45)[a]	95 (68)[a]	100 (99)	100 (100)
multiplicity (outer shell)	4.4 (1.8)	3.7 (2.3)	3.1 (1.6)	3.7 (3.7)
Refinement				
no. of protein atoms	2491	2370	2964	3036
no. of solvent atoms	380	273	354	423
no. of oligosaccharide atoms	not applicable	36	not applicable	23
R_{cryst}	0.12	0.15	0.17	0.14
R_{free}	0.17	0.19	0.20	0.16
mean B for protein atoms (Å^2)	14	20	20	16
mean B for solvent atoms (Å^2)	26	33	31	31
mean B for oligosaccharide atoms (Å^2)	not applicable	34	not applicable	16
rmsd for 1−2 bonds (Å)	0.018	0.021	0.009	0.006
rmsd 1−3 angles (deg)	1.5	1.6	1.1	1.06
Ramachandran statistics (% favored/allowed regions calcuated using COOT)	95.5/3.5	95.3/4.3	98.9/1.6	98.1/1.4
PDB entry	2WHJ	2WHL	2WHK	2WHM

[a] High-resolution incompleteness reflects integration into the corners of a square detector with the penultimate shell >95% complete in each case.

Table 3: Biochemical Properties of GH5 and GH26 Mannanases[a]

	Man_3	Man_4	Man_5	Man_6	galactomannan			glucomannan			ivory nut mannan		
enzyme	k_{cat}/K_M	k_{cat}/K_M	k_{cat}/K_M	k_{cat}/K_M	k_{cat}	K_M	k_{cat}/K_M	k_{cat}	K_M	k_{cat}/K_M	k_{cat}	K_M	k_{cat}/K_M
*Ba*Man5A	5.3×10^{-5}	1.4×10^{-1}	1.5×10	1.2×10^{2}	3.8×10^{4}	1.8	1.5×10^{4}	4.5×10^{4}	2.6	2.6×10^{4}	3.0×10^{4}	2.8	1.1×10^{4}
*Bs*Man26A	1.3×10^{-3}	2.8×10^{-1}	4.4	2.4×10	3.3×10^{2}	4.5	7.3×10	3.5×10^{2}	2.7	1.3×10^{2}	1.5×10^{2}	6.8	2.2×10
*Cf*Man26A[b]	1.9×10^{-2}	3.7×10^{-1}	2.7	6.7	3.6×10^{4}	2.3	1.6×10^{4}	ND[c]	ND[c]	ND[c]	ND[c]	ND[c]	ND[c]
*Cj*Man26A[b]	1.8	1.4×10	ND[c]	2.8×10	2.8×10^{5}	3.2	8.9×10^{4}	4.0×10^{5}	2.8	1.5×10^{5}	ND[c]	ND[c]	ND[c]
*Cj*Man5A[b]	1.5×10^{-5}	3.9×10^{-3}	1.4×10	2.8	1.4×10^{5}	8.5	1.5×10^{4}	6.2×10^{4}	6.2	1.0×10^{4}	NA[d]	NA[d]	NA[d]

[a] The units of the kinetic parameter k_{cat}/K_M for the mannooligosaccharides are $min^{-1}\ \mu M^{-1}$. The units of the kinetic parameters for the polysaccharide substrates are as follows: k_{cat}, min^{-1}; K_M, mg mL^{-1}; k_{cat}/K_M, mL min^{-1} mg^{-1}. [b] The biochemical properties of *Cf*Man26A (*32*) and *Cj*Man5A (*10*) were reported previously. The activities of *Cj*Man26A against the mannooligosaccharides were also reported previously (*21*), but the activity of the enzyme against polysaccharides is reported here. [c] Not determined. [d] No activity detected.

against mannotetraose (Man_4). In both enzymes, the ratio of the hydrolysis products ([Man_2]:[Man_1 + Man_3]) reports on the productive binding energy associated with substrate binding at the −3 and +2 subsites (which was ∼2:1) (Figure 2), when compared to the rate of Man_3 hydrolysis, which binds from the −2 to the +1 subsite. Thus, the $\Delta G^{\ddagger}$ values associated with Man binding at the −3 and +2 subsites of *Bs*Man26A are −1.6 and −3.3 kcal/mol, respectively, while the equivalent values for *Ba*Man5A are −1.2 kcal/mol (−3 subsite) and 2.2 kcal/mol (+2 subsite), respectively. Thus, in *Bs*Man26A and *Ba*Man5A, both the −3 and +2 subsites contribute significantly to the increased activity displayed by the two enzymes for the tetrasaccharide, compared to that of the trisaccharide. *Bs*Man26A and *Ba*Man5A exhibit ∼10- and 100-fold increases in activity for mannopentaose, respectively, compared to Man_4. Notably, *Bs*Man26A released significant quantities of Man_1 and Man_4, in addition to the expected Man_2 and Man_3 (Figure 2), demonstrating that the enzyme likely contains four negative substites (−4 to −1), although binding to the −4 subsite is weaker than binding to the +2 subsite with a $\Delta\Delta G^{\ddagger}$ of −1.8 kcal/mol. The 10-fold higher activity of *Ba*Man5A for M_6, compared to M_5, suggests that the enzyme, similar to *Bs*Man26A, contains six subsites, although it is possible that the distal positive subsite displays a preference for an internal Man that is maintained in its β conformation through linkage to an adjacent sugar.

Exploring the Recognition of Glc in the Substrate Binding Cleft of Mannanases. To explore in more detail the specificity of the −2 and +1 subsites for Glc and Man, the nature of the reaction products released from glucomannan was analyzed; the production of Glc-Man as a significant reaction product shows that the enzyme can accommodate Glc at both the −2 and +1 subsites. The data here show that the ratio of Glc-Man to Man_2 generated by *Ba*Man5A and *Cj*Man5A during the initial stages of hydrolysis was >1, indicating that both enzymes display a preference for Glc at the −2 and/or +1 subsites (Figure 3). Hydrolyzing glucomannan to completion with *Cj*Man5A generated ∼20% more Man_2 than Glc-Man, indicating that the ratio of initial products is not a reflection of more Glc-Man

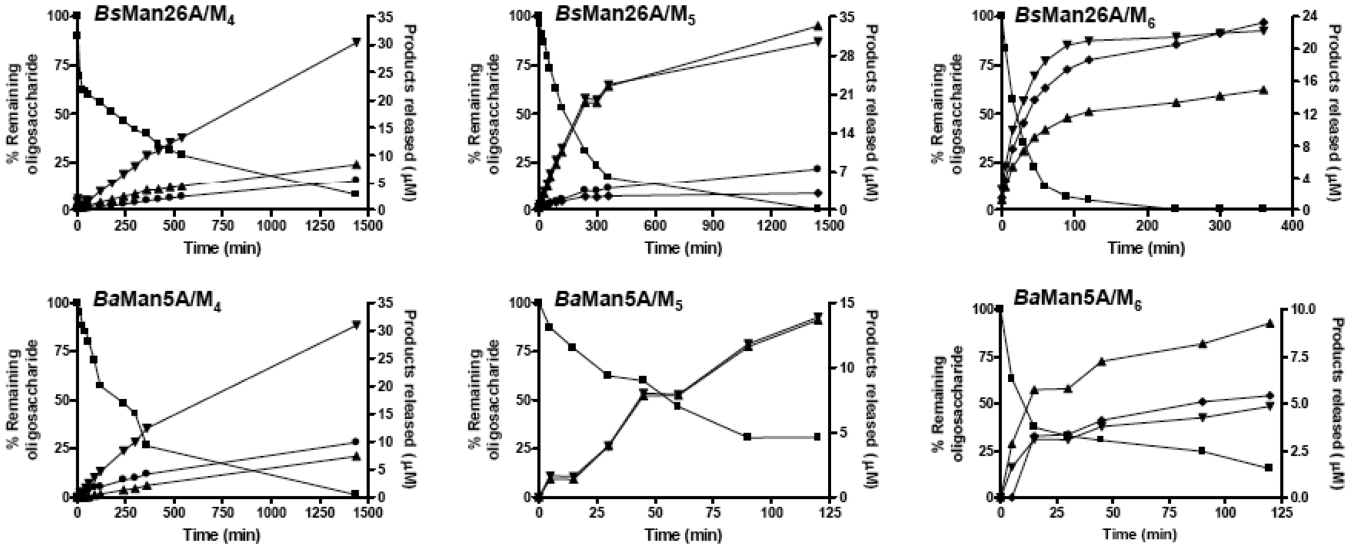

FIGURE 2: Products of oligosaccharide hydrolysis by bacterial mannanases. The percent of remaining substrate (■) is plotted on the left and the concentration of product released on the right: Man_1 (●), Man_2 (▼), Man_3 (▲), and Man_4 (◆).

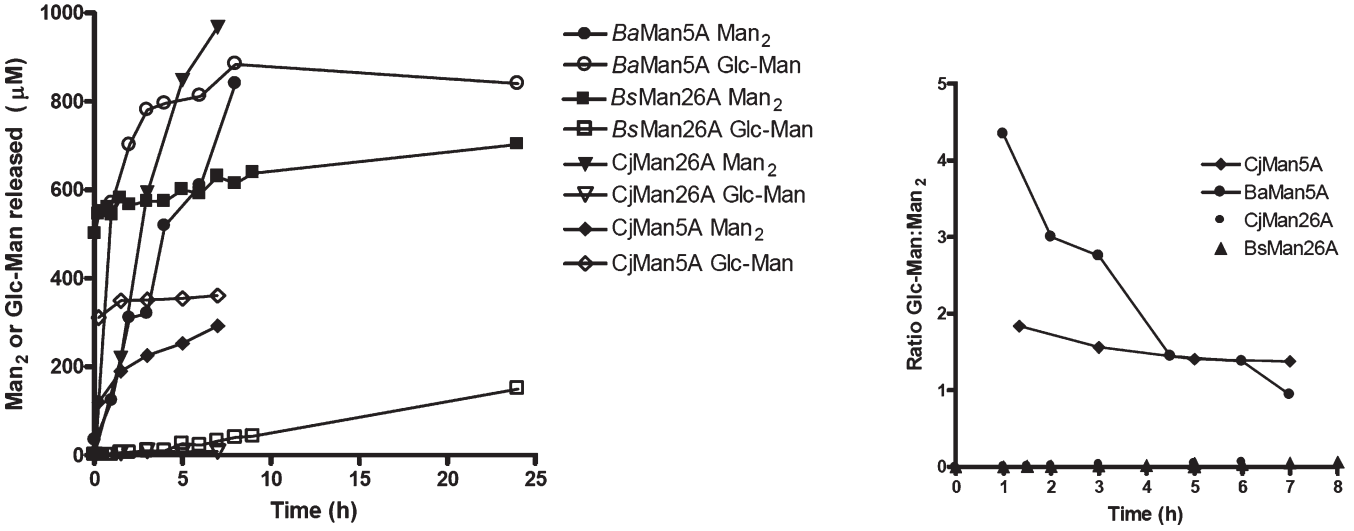

FIGURE 3: Release of Man_2 and Glc-Man from glucomannan by GH5 and GH26 mannanases. Glucomannan (2 mg/mL) was incubated with the indicated enzyme in 50 mM sodium phosphate/12 mM citrate buffer, and at timed intervals, the quantity of Man_2 and Glc-Man was determined by HPLC: (left) amounts of Man_2 and Glc-Man released and (right) ratios of the two disaccharides.

than Man-Man linkages in the substrate. In contrast, the two GH26 mannanases generated very little Glc-Man compared to Man_2, and in the case of *Bs*Man26, the heterodisaccharide was only evident after 24 h (Figure 3). These data indicate that the two GH26 enzymes exhibit a strong preference for Man at the proximal subsites; however, it is unclear whether the specificity for this sugar is conferred by the −2 or +1 subsites. To explore this issue, we assessed the activity of *Cj*Man26A against aryl glycosides 4NPManGlc and $4NPMan_2$. The data show that the enzyme displays ~1×10^4-fold higher activity for $4NPMan_2$ [k_{cat}/K_M = 5.3 min^{-1} mM^{-1} (Table 4)] than for 4NPManGlc (k_{cat}/K_M = 2.0×10^{-4} min^{-1} mM^{-1}), demonstrating that the −2 subsite of this GH26 mannanase certainly exhibits very tight specificity for Man.

Structural Basis for Man Specificity in the −2 Subsite of CjMan26A. Previous data had revealed the structure of *Cj*Man-26A in complex with substrates and mechanism-based inhibitors in which the −2 subsite is occupied with Man (*15*). Here, the structure of the *Cj*Man26A E121A/E320G variant was determined in complex with Man_2 (Figure 4). In past work, it was clear that O6 of the −2 sugar made a hydrogen bond with the carboxylate of Glu-121, His-377 made a single polar contact with O2, and Arg-361 interacted with both O2 and O3 through three hydrogen bonds. To explore the contribution of these residues to substrate binding, and Man specificity in particular, we evaluated the catalytic properties of the −2 variants H377A, R361A, E121A, and R361A/H377A. The data (Table 4) show that the E121A mutant is approximately 100-fold less active than wild-type *Cj*Man26A against both oligosaccharides and polysaccharides. While the H377A mutation also caused an ~100-fold decrease in the activity of the mannanase against M_4 and $4NPMan_2$, the mutant hydrolyzed polysaccharides only 10−20-fold less efficiently than did the wild-type enzyme. Substitution of Arg-361 with alanine caused a 3000-fold decrease in activity against oligosaccharides, while the reduction in the rate of polysaccharide hydrolysis was more modest, ranging from 700- to 900-fold. The double mutant R361A/H377A was, not surprisingly, the least active mutant, although its differential activity against polysaccharides and oligosaccharides was less evident than that of its progenitors with single amino acid

Table 4: Catalytic Activities of the Wild Type and Variants of *Cj*Man26A[a]

	Man_4	$4NPMan_2$			azo-galactomannan			galactomannan			glucomannan		
*Cj*Man26A	k_{cat}/K_M	k_{cat}	K_M	k_{cat}/K_M	k_{cat}	K_M	k_{cat}/K_M	k_{cat}	K_M	k_{cat}/K_M	k_{cat}	K_M	k_{cat}/K_M
wild type	3.3	3.9	7.2×10^{-1}	5.3	9.1×10^4	0.5	1.9×10^5	2.8×10^5	3.2	8.9×10^4	4.0×10^5	2.8	1.5×10^5
E121A	3.0×10^{-2}	ND[b]	ND[b]	8.5×10^{-2}	2.3×10^3	2.6	8.6×10^2	ND[b]	ND[b]	5.1×10^2	ND[b]	ND[b]	8.5×10^2
R361A	1.2×10^{-3}	ND[b]	ND[b]	1.0×10^{-3}	6.5×10^2	3.0	2.2×10^2	ND[b]	ND[b]	1.3×10^2	ND[b]	ND[b]	1.4×10^3
H377A	4.1×10^{-2}	ND[b]	ND[b]	7.1×10^{-2}	3.3×10^4	1.7	2.0×10^4	ND[b]	ND[b]	6.4×10^3	ND[b]	ND[b]	7.6×10^3
R361A/H377A	1.0×10^{-4}	ND[b]	ND[b]	2.0×10^{-4}	1.2×10^2	3.1	3.8×10	ND[b]	ND[b]	1.6×10	ND[b]	ND[b]	8.3×10

[a] The units of the kinetic parameter k_{cat}/K_M for Man_4 are $min^{-1}\ \mu M^{-1}$. The units for the kinetic parameters for $4NPMan_2$ are as follows: k_{cat}, min^{-1}; K_M, mM; k_{cat}/K_M, $min^{-1}\ mM^{-1}$. The units for the kinetic parameters for the polysaccharide substrates are as follows: k_{cat}, min^{-1}; K_M, mg mL^{-1}; k_{cat}/K_M, mL min^{-1} mg^{-1}. [b] Individual kinetic constants could not be measured as the maximum concentration of soluble substrate was much lower than K_M.

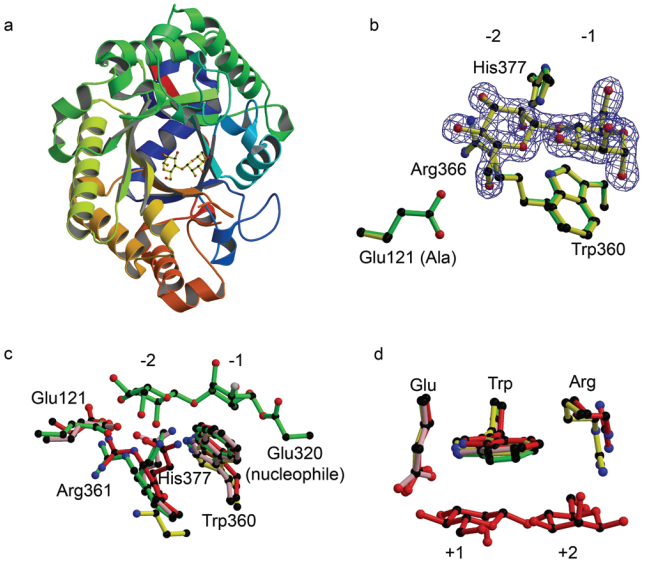

FIGURE 4: Structure of *Cj*Man26A and comparison of subsites and their specificities. (a) Three-dimensional structure cartoon of *Cj*Man-26A [E121A/E360G Man_2 complex (this work)], color-ramped from the N-terminus (blue) to the C-terminus (red) with the ligand in ball-and-stick representation. (b) Electron density ($2F_{obs} - F_{calc}$ at 1σ) for Man_2 bound in the −1 and −2 subsites of *Cj*Man26A (E121A/E360G variant colored yellow) overlaid with the protein atoms only of wild-type C*j*Man26A (green). (c) Overlay of the −1 and −2 subites of *Cj*Man26A (mannobiosyl-enzyme intermediate, PDB entry 1GW1, colored green) with *Bs*Man26A (this work, colored), *Cj*Man26C ((*14*), colored red), and *Cf*Man26 (PDB entry 2BVT, pink). The numbering is for the *Cj*Man26A enzyme. (d) Overlay of the +1 and +2 subites of *Cj*Man26C (PDB entry 2VX6, red) with *Cj*Man26A (PDB entry 1GW1, green), *Cf*Man26 (PDB entry 2BVT, pink), and *Bs*Man26A (this work, yellow).

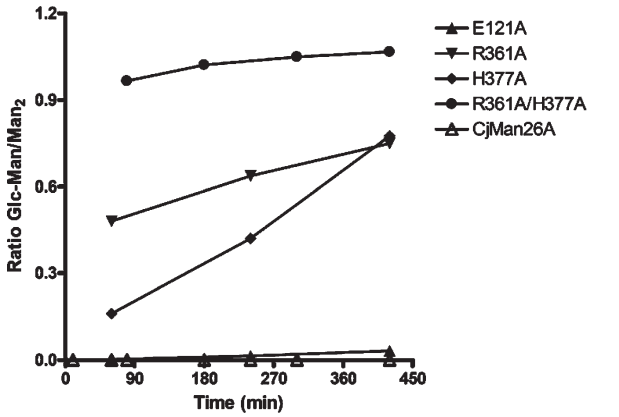

FIGURE 5: Release of Man_2 and Glc-Man from glucomannan by variants of *Cj*Man26A. Glucomannan (2 mg/mL) was incubated with the indicated enzyme in 50 mM sodium phosphate/12 mM citrate buffer, and at timed intervals, the quantity of Man_2 and Glc-Man was determined by HPLC.

changes. The decrease in catalytic efficiency reflects a substantial increase in K_M against the polysaccharides; indeed, the poor solubility of galactomannan and glucomannan precluded the determination of this kinetic parameter. These data support the structural data in showing that Arg-361, His-377, and Glu-121 all make important productive polar interactions with Man at the −2 subsite, although the arginine, through its multiple interactions with O2 and O3, makes the most significant contribution to substrate binding.

The observation that the R361A and H377A mutations appeared to have a larger influence on the activity of the enzyme against oligosaccharides, than against polysaccharides, is consistent with previous studies showing a similar differential effect of amino acid substitutions in glycoside hydrolases, including *Cj*Man26A (*20*, *21*, *27*−*30*). Indeed, the importance of O2 and O3 recognition (Arg-361 interacts with O2 and O3, while His-377 contacts O2) in oligosaccharide hydrolysis, as opposed to polysaccharide cleavage, is evident in other glycoside hydrolases (*20*, *27*). It is evident that most, although not all (*28*−*30*), of these mutations cluster around proximal subsites −2 and +1 (*20*, *21*, *27*).

To explore how the −2 mutations influenced the capacity of *Cj*Man26A to accommodate Glc, the mutant enzymes were incubated with glucomannan and the reaction products were analyzed. The data show (Figure 5) that E121A releases very little Glc-Man, indicating that the mutation does not cause reduce the specificity at the −2 subsite, consistent with the interaction of Glu-121 with O6. In contrast, there was a substantial change in the product profile generated by H377A, R361A, and, in particular, H377A/R361A. All three mutants produced substantially more Glc-Man than the wild-type enzyme, and indeed, the double mutant did not appear to distinguish between Man and Glc. It should be emphasized, however, that removal of the His and Arg residues did not improve Glc access but simply removed the polar interactions with the axial O2 atom of Man that favor that substrate.

To investigate the structural features of the *Cj*Man26A mutants, which facilitated accommodation of Glc at the −2 subsite, inactive forms of the three variants were generated by the introduction of the catalytic nucleophile mutation E320G. The resultant proteins were cocrystallized with both 4NPManGlc and Man_4. Crystal structures of all these proteins were determined. However, neither 4NPManGlc nor Man_4 was present in the crystal structures of E320G/R361A, E320G/H377A, and E320G/R361A/H377A (data not shown). Indeed, the loop containing the

mutant residues was disordered, and thus, it is not possible to provide fine detail of the topology of the −2 subsite in these *Cj*Man26A variants (not shown). While the E320A mutant did contain 4NPManGlc, the aryl group was located in the −1 subsite and Man in the −2 subsite, emphasizing the tight specificity of this distal negative subsite for Man (data not shown). The *Cj*Man26A E212A/E320G variant, crystallized with Man_4 did contain Man in the −2 subsite (by virtue of an ordered mannobiosyl moiety in the −2 and −1 subsites) (Figure 4b). The conformation of the −2 subsite in the mutant was identical to that of the wild-type mannanase (in complex with ligand), confirming that the loss of the O6 enzyme interaction, rather than any major structural perturbation, was responsible for the decrease in activity.

Crystal Structures of BaMan5A and BsMan26A. To explore the structural basis for the biochemical properties displayed by the two *Bacillus* mannanases, their crystal structures were determined (Figure 6). Despite considerable crystallization efforts, the structure of the GH26 enzyme could be obtained only in apo form while that of the GH5 mannanase was determined in both apo form and (through a serendipitous mutant more amenable to complex formation) with Man_3 bound at subsites −4 to −2 in which with each Man adopts a relaxed $^4C_1$ conformation. Consistent with their location in the GH-A clan, both enzymes display a canonical $(\alpha/\beta)_8$-fold barrel in which the catalytic acid−base and nucleophile glutamates are at the end of β-strands 4 and 7, respectively (*3*, *31*) (Figure 6a,b). Overlaying the structure of the *Bacillus* enzymes with other GH26 and GH5 mannanases provides insight into the structural basis for the substrate specificities displayed by these enzymes, with respect to both their hydrolysis of manno-configured substrates and their capacity to accommodate Glc in subsites distal to subsite −1.

(i) The −1 Subsite. Superimposition of the −1 subsite in the GH5 (Figure 6c) and GH26 (Figure 6d) mannanases reported here reveals a striking degree of structural conservation. The location of the two critical catalytic residues is conserved in both families (Figure 6d). The invariant His in GH26 enzymes (His-211 in *Cj*Man26A and His-166 in *Bs*Man26A), which interacts with O2, is replaced with an Asn in the GH5 enzymes (Asn-127 in *Ba*Man5A); however, the side chains of both polar residues are in an appropriate position to interact with O2 of Man, when it adopts its pseudoequatorial orientation along the reaction coordinate (*14*−*16*). In addition, the pseudoaxial O3 atom, induced by the conversion of Man from its $^4C_1$ geometry along its $^1S_5$ to $^OS_2$ migration, makes a polar interaction with a highly conserved histidine (His-143, His-105, and His-88 in *Cj*Man26A, *Bs*Man26A, and *Ba*Man5A, respectively). Finally, the −1 subsite contains a hydrophobic platform (Trp-360, Trp-298, and Trp-251 in *Cj*Man26A, *Bs*Man26A, and *Bs*Man5A, respectively) that makes extensive hydrophobic interactions with the pyranose ring of the Man.

(ii) The −2 Subsite of GH26 Enzymes. Overlaying the −2 subsite regions of the *C. japonicas* enzymes *Cj*Man26A and *Cj*Man26C, the *Cellulomonas fimi* mannanase *Cf*Man26A (*32*) (Figure 6c,d), and comparing these overlays with *Bs*Man26A reveal significant differences that could explain the variation in activity displayed by these glycoside hydrolases for small mannooligosaccharides. It is difficult to accurately predict the interactions between *Bs*Man26A and the sugar at the −2 subsite (and the −3 subsite), as the accommodation of a mannan chain might require conformational changes to the extended loops 2 and

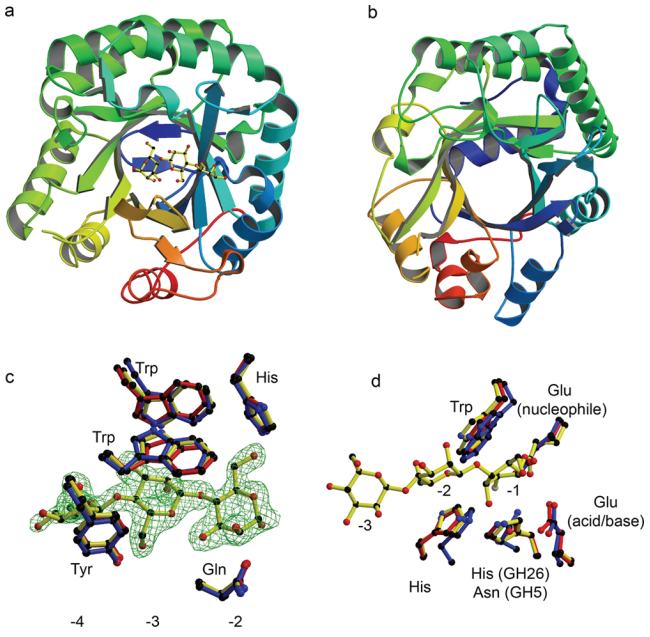

FIGURE 6: Crystal structures of *Ba*Man5A and *Bs*Man26A. (a) Crystal structure of BaMan5A, color-ramped from the N-terminus (blue) to the C-terminus (red) with Man_3 in ball-and-stick representation. (b) Three-dimensional structure of *Bs*Man26A, color-ramped from the N-terminus (blue) to the C-terminus (red). (c) Electron density ($2F_{obs} - F_{calc}$ at 1σ) for Man_3 bound in the −2 to −4 subsites of *Ba*Man5 (Y8F variant colored yellow) overlaid with *Trichoderma reesei* Man5A (blue) and Man5 from *Bacillus* sp. (PDB entry 1WKY; red). (d) Overlay of GH5 and GH26 mannanases in the negative subsites. *Cj*Man26A (trapped mannotriosyl-enzyme intermediate, PDB entry 1GVY, colored yellow) with *Ba*Man5A (blue, this work) and *Bs*Man26A (red, this work).

4. Nevertheless, it is likely that Tyr-40, which is spatially equivalent to Glu-121 in *Cj*Man26A, will also make a polar contact with O6 of the Man at the −2 subsite, while Phe-116, which is structurally equivalent to Trp-162 in the *Cellvibrio* enzyme, will make hydrophobic contacts with the pyranose ring. The strong polar interactions between *Cj*Man26A and O2 and O3 of the −2 sugar will, however, be less evident in *Bs*Man26A, where His-377 is replaced with Asp-300 and Arg-361 with Asn-299. Although Asn-299 is likely too distant from the bound sugar to make a polar contact, it is possible that Asp-300 makes hydrogen bonds to O2, providing an explanation for why *Bs*Man26A is also selective for Man at the −2 subsite. In *Cf*Man26A, the residues equivalent to *Cj*Man26A His-377 and Glu-121 are Gln-329 and Glu-78, respectively, which make polar contacts with O2 (Gln-329) and O6 (Glu-78) of the Man at the −2 subsite, but the amino acid corresponding to *Cj*Man26A Arg-361 in the *Cellulomonas* enzyme is Phe-325. Current structural data, therefore, indicate that at the −2 subsite polar residues, corresponding to Asp-300 in *Bs*Man26A, make a hydrogen bond with the axial O2 atom of Man, and this interaction confers specificity for Man, which is likely to be a general but not universal feature of GH26 mannanases. Indeed, a previous study showed that a third GH26 *C. japonicus* mannanase, *Cj*Man26B, is able to accommodate Glc at the −2 and +1 subsites (*10*) which likely reflects the lack of sequence conservation with *Cj*Man26A or *Cj*Man26C in the loop that forms the −2 subsite. It is also evident that Arg-361 in *Cj*Man26A and the equivalent residue, Arg-374, in *Cj*Man26C mediate tight binding of the substrate at the −2 subsite, resulting in the extremely high activity displayed by the two *Cellvibrio* enzymes for small

mannooligosaccharides (*14*, *21*). Thus, we predict that other GH26 mannanases, which contain an arginine equivalent to Arg-361 in *Cj*Man26A will display similarly elevated activity against small substrates.

(iii) The −2 Subsite of GH5 Enzymes. In contrast to the −1 subsite, there is little similarity between the −2 subsites of GH26 and GH5 mannanases. The Man at the −2 subsite of *Ba*Man5A makes several hydrophobic interactions with the enzyme, notably with Trp-31 but also with Trp-61 and Trp-251. In addition, O6 makes polar contacts with Nε2 of His-88, O3 forms hydrogen bonds to the N atom of Ser-257, and O2 may make a polar contact with Oδ1 of Asn-256. It is evident, however, that the −2 subsite of *Ba*Man5A displays a preference for Glc over Man, indicating that O2 in an equatorial configuration is also able to make polar contacts (stronger than in an axial conformation) with the enzyme, most likely also with Asn-256.

The −2 subsites of *Ba*Man5A and the other two bacterial enzymes for which a crystal structure has been determined, *Bj*Man5A from *Bacillus* sp. JAMB-602 [PDB entry 1WKY (*33*)] and *Thermobifida fusca Tf*Man5A [PDB entry 3MAN (*34*)], are extremely similar. Indeed, the residues that interact with the sugar through their side chains are invariant in these three enzymes. It has been proposed that the residue equivalent to *Ba*Man5A Asn-256 in *Tf*Man5A (Asn-259) confers specificity for mannan (*34*). The *Bacillus* enzyme, however, displays a preference for Glc, over Man, at the −2 subsite, and thus, it is unlikely that the conserved Asn contributes to mannan specificity (see above). Furthermore, sequence alignments show that these key substrate binding residues are conserved in *Cj*Man5A, explaining why the *Cellvibrio* enzyme also does not display a preference for Man at this subsite. While there is less structural conservation between *Ba*Man5A and eukaryotic GH5 mannanases, *B*aMan5A His-88 and Asn-256 are conserved in two of the enzymes, *Mytilus edulis* Man5A (*35*) and *Lycopersicon Le*Man4A (*36*), whereas Asn-256 is replaced with an Asp in *Hypocrea jecorina Hj*Man5A (*37*). It is likely, therefore, that in the GH5 mannanases, for which structural data are available, the critical −2 subsite does not display specificity for Man but may well indeed exhibit a preference for Glc.

(iv) Distal Negative Subsites. Biochemical data show that both *Bs*Man26A and *Ba*Man5A contain functional, albeit "weak", −3 and −4 subsites. Accommodation of Man at the −3 subsite would require conformational changes to prevent steric clashes with Trp-72 and Asp-40, although it remains likely that these residues, in addition to Tyr-40, which is parallel to the pyranose ring, interact with the sugar at the −3 subsite. The only residues that could interact with Man at a potential −4 subsite, as far as we can judge, are Arg-69 and Leu-73.

The interactions between the substrate and *Ba*Man5A at the −3 subsite are through hydrophobic interactions with Trp-31 and Trp-61, while the sugar at the −4 subsite makes apolar contacts with Tyr-32. All three hydrophobic residues are invariant in the structures of the two other bacterial GH5 mannanases, revealing that all these enzymes contain essentially identical negative subsites extending from subsite −4 to −1. There appear to be no polar interactions between the substrate and the enzyme at subsites −3 and −4, suggesting that there is no specificity for Glc or Man. It is possible, however, that an equatorial O2 atom at the −3 and/or −4 subsites may make productive polar contacts or steric clashes with the protein, which would confer selectively for Glc or Man.

(v) Positive Subsites of BsMan26A and BaMan5A. The positive subsites of *Bs*Man26A span approximately 12 Å and thus probably accommodate two sugars. Overlaying the structure of *Cj*Man26C, which has Man bound at the +1 and +2 subsites, provides insight into the likely mechanism by which this region of the active site of several GH26 mannanases recognizes substrate (Figure 4d). Thus, *Ba*Man5A Trp-172, which is invariant in all other known mannanase structures, makes planar hydrophobic interactions with the sugar at the +1 subsite. Asp-218 in the *Bacillus* enzyme, equivalent to Asn-257 in *Cj*Man26A, makes a weak polar contact with O6, but there are no interactions with O2, suggesting that the +1 subsite may not discriminate between Glc and Man. There is considerably less conservation at the +2 subsite between the GH26 enzymes. In *Bs*Man26A, Arg-221, equivalent to Arg-269 in *Cj*Man26C, is likely to make polar contacts with the sugar, including the axial O2 atom. Thus, the basic residue not only provides the majority of the substrate binding energy at this distal positive site but also displays specificity for Man. Indeed, this arginine appears to confer the tight binding evident in the +2 subsites of *Bs*Man26A and *Cj*Man26C, and the lack of an equivalent residue in *Cj*Man26A and *Cf*Man26A explains why the +2 subsite in these enzymes interacts only weakly with the substrate. Thus, the analysis of the structure allows prediction of the following substrate specificities of the four GH26 mannanases for structures within glucomannan: *Bs*Man26A and *Cj*Man26C, ManMan(Man/Glc)Man; *Cj*Man26A and *Cf*Man26A, ManMan(Man/Glc)(Man/Glc).

In the +1 subsite, a hydrophobic platform, Trp-164 in the case of *Ba*Man5A, is predicted to interact with substrate (on the basis of its similarity with *Hj*Man5A). There are no direct polar interactions with the +1 sugar, indicting that the enzyme does not display specificity for Glc or Man at this subsite. Indeed, comparing *Ba*Man5A with all other known GH5 mannanase structures shows that Trp-164 is invariant and, similarly, none of the enzymes interact with O2, although they do make hydrogen bonds with other hydroxyls in the sugar. As in GH26 mannanases, the +2 subsite is not highly conserved in the GH5 mannanases. The only interaction between *Ba*Man5A and the +2 subsite sugar is through a polar contact between the OH group of Tyr-196 and O1 of the Man. By contrast, *Hj*Man5A and *Tf*Man5A make several polar interactions with the +2 sugar, including the axial O2 atom, conferring specificity for Man. Downstream of the +2 subsite, two aromatic residues, Tyr-196 and Trp-132, are likely to make hydrophobic contacts with the substrate at the +3 subsite. Indeed, the hydrophobic platform provided by Trp-132 in *Ba*Man5A is conserved in other GH5 mannanases, indicating that a functional +3 subsite is a common feature of these enzymes.

CONCLUSIONS

This report provides structural insight into the complex substrate specificities displayed by β-mannanases. Biochemical studies point to a divergence in specificity between GH5 and GH26 mannanases. It would appear that the GH5 mannanases are able to accommodate, and even make productive interactions with, Glc at the −2 and +1 subsites. Thus, these enzymes are able to hydrolyze mannosidic linkages that are flanked by Man or Glc. Similarly, at the distal negative subsites, −3 and −4, O2 does not make polar contacts with the enzyme, while in *Ba*Man5A, the positive region of the substrate binding cleft also does not harness axial O2 groups as specificity determinants. Thus, while

*Ba*Man5A hydrolyzes only mannosidic bonds, because of its absolute specificity for Man at the −1 subsite (a feature that is invariant in all mannanases), it would appear that the topographical features of the substrate binding cleft of this enzyme are optimized to utilize glucomannan as its preferred substrate. The relaxed specificity for Glc or Man, apart from the critical −1 subsite, is a feature shared with the other GH5 mannanases, where structural information is available.

One may extend the gluco versus manno comparison even further for GH5 as this family contains enzymes with a variety of substrate specificities, in addition to mannanases, including endoglucanases (cellulases) active on β-1,4-linked glucopyranoside polysaccharides. At the topographical level, the *B. agaradhaerens* Man5A and the endoglucanase Cel5A from the same bacterium (*38*, *39*) are extremely similar with long open grooves evolved to accommodate linear glucan substrates, β-1,4-mannoside- and β-1,4-glucoside-based, respectively. As mentioned previously, their −1 subsite catalytic apparatus is also highly conserved, and again, it is not in the vicinity of O2 where the enzyme environments differ but around O3, a facet which we have mentioned previously in the context of GH5 and GH26 (*14*, *15*, *40*, *41*). The cellulase versus mannanase comparison thus adds to the overall picture that distal subsite recognition favors appropriate aromatic platforms and H-bonding designed to accommodate the axial or equatorial O2 hydroxyls of mannose or glucose, as required, whereas in the −1 subsite, the enzymes have evolved to bind the similarly pseudoequatorial O2 atom of either Man or Glc (when distorted at their appropriate transition states) and that specificity at this site derives instead from the interactions of O3 which facilitate the equatorial O3 atom of glucose in the cellulases but the pseudoaxial (but identically configured in the ground state) geometry in the distorted mannoside.

In contrast, the GH26 mannanases, characterized to date, generally display tight specificity for Man at both the −2 subsite, by selecting the axial O2 atom as a key specificity determinant, and the −1 subsite, where substrate recognition is not conferred by the ground state structure of the sugar but by the pseudoequatorial O2 conformation adopted by Man along the reaction coordinate. The conservation of a polar residue, equivalent to *Cj*Man26A His-377, in GH26 enzymes indicates that Man recognition at the −2 subsite is a general, but not invariant, feature within this family. In addition, this report has also revealed that an arginine, present in the −2 subsite of two GH26 mannanases, confers unusually high activity against small mannooligosaccharide substrates. Screening genomic databases for other GH26 enzymes that retain this arginine may facilitate the identification of novel mannooligosaccharidases. Currently, the two *Cellvibrio* enzymes that contain a high-affinity −2 subsite do not possess additional negative binding subsites, which may explain why the high activity displayed against Man_3 and Man_4 is not translated to the hydrolysis of polysaccharides. The structural data presented will be used to guide protein engineering strategies that either introduce the "high-affinity arginine" into selected GH26 mannanases that contain an extended substrate binding cleft or build additional subsites into enzymes that already contain the basic residue at the −2 subsite. It is possible that these engineered enzymes may display elevated activities against mannan and glucomannan and thus add to the toolkit of biocatalysts deployed within the bioenergy and bioprocessing industries.

In conclusion, this report provides the structural basis for Glc and Man recognition in β-mannanases. GH5 mannanases appear to display relaxed specificity for Glc or Man at the majority of the subsites and thus are optimized for glucomannan attack. By contrast, GH26 mannanases, by selecting Man at both the −1 and −2 subsites, preferentially attack homopolymers of Man. As glucomannan is generally found in the cell walls of angiosperms while mannan is often a storage polymer in seeds, it would appear that GH5 mannanases target plant cells, which is consistent with the presence of cellulose-specific noncatalytic carbohydrate binding modules in many of these enzymes (*10*). In contrast, GH26 enzymes lack cellulose-specific CBMs and are often tethered to the bacterial cell wall (*42*), indicating that their primary substrates are mannooligosaccharides or soluble mannans such as galactomannans.

ACKNOWLEDGMENT

The staff of the European Synchrotron Radiation Facility (ESRF) is thanked for the continuing provision of data collection facilities. Marek Brzozowski and past members of the Davies group are thanked for contributions to this project, and Carlos Martinez-Fleites is thanked for help with figure preparation.

REFERENCES

1. Ragauskas, A. J., Williams, C. K., Davison, B. H., Britovsek, G., Cairney, J., Eckert, C. A., Frederick, W. J. Jr., Hallett, J. P., Leak, D. J., Liotta, C. L., Mielenz, J. R., Murphy, R., Templer, R., and Tschaplinski, T. (2006) The path forward for biofuels and biomaterials. *Science 311*, 484–489.
2. Cantarel, B. L., Coutinho, P. M., Rancurel, C., Bernard, T., Lombard, V., and Henrissat, B. (2009) The Carbohydrate-Active EnZymes database (CAZy): An expert resource for Glycogenomics. *Nucleic Acids Res. 37*, D233–D238.
3. Henrissat, B., Callebaut, I., Fabrega, S., Lehn, P., Mornon, J. P., and Davies, G. (1995) Conserved catalytic machinery and the prediction of a common fold for several families of glycosyl hydrolases. *Proc. Natl. Acad. Sci. U.S.A. 92*, 7090–7094.
4. DeBoy, R. T., Mongodin, E. F., Fouts, D. E., Tailford, L. E., Khouri, H., Emerson, J. B., Mohamoud, Y., Watkins, K., Henrissat, B., Gilbert, H. J., and Nelson, K. E. (2008) Insights into plant cell wall degradation from the genome sequence of the soil bacterium *Cellvibrio japonicus*. *J. Bacteriol. 190*, 5455–5463.
5. Martinez, D., Berka, R. M., Henrissat, B., Saloheimo, M., Arvas, M., Baker, S. E., Chapman, J., Chertkov, O., Coutinho, P. M., Cullen, D., Danchin, E. G., Grigoriev, I. V., Harris, P., Jackson, M., Kubicek, C. P., Han, C. S., Ho, I., Larrondo, L. F., de Leon, A. L., Magnuson, J. K., Merino, S., Misra, M., Nelson, B., Putnam, N., Robbertse, B., Salamov, A. A., Schmoll, M., Terry, A., Thayer, N., Westerholm-Parvinen, A., Schoch, C. L., Yao, J., Barabote, R., Nelson, M. A., Detter, C., Bruce, D., Kuske, C. R., Xie, G., Richardson, P., Rokhsar, D. S., Lucas, S. M., Rubin, E. M., Dunn-Coleman, N., Ward, M., and Brettin, T. S. (2008) Genome sequencing and analysis of the biomass-degrading fungus *Trichoderma reesei* (syn. *Hypocrea jecorina*). *Nat. Biotechnol. 26*, 553–560.
6. Xu, J., Bjursell, M. K., Himrod, J., Deng, S., Carmichael, L. K., Chiang, H. C., Hooper, L. V., and Gordon, J. I. (2003) A genomic view of the human-*Bacteroides thetaiotaomicron* symbiosis. *Science 299*, 2074–2076.
7. Brett, C. T., and Waldren, K. (1996) Physiology and Biochemistry of Plant Cell Walls. Topics in Plant Functional Biology , Vol. 1, Chapman and Hall, London.
8. Gilbert, H. J., Stalbrand, H., and Brumer, H. (2008) How the walls come crumbling down: Recent structural biochemistry of plant polysaccharide degradation. *Curr. Opin. Plant Biol. 11*, 338–348.
9. McCleary, B. V. (1988) Carob and guar galactomannans. *Methods Enzymol. 160*, 523–527.
10. Hogg, D., Pell, G., Dupree, P., Goubet, F., Martin-Orue, S. M., Armand, S., and Gilbert, H. J. (2003) The modular architecture of *Cellvibrio japonicus* mannanases in glycoside hydrolase families 5 and 26 points to differences in their role in mannan degradation. *Biochem. J. 371*, 1027–1043.

11. Davies, G., and Henrissat, B. (1995) Structures and mechanisms of glycosyl hydrolases. *Structure 3*, 853–859.
12. Vocadlo, D., and Davies, G. J. (2008) Mechanistic Insights into Glycosidase Chemistry. *Curr. Opin. Chem. Biol. 12*, 539–555.
13. Davies, G. J., Wilson, K. S., and Henrissat, B. (1997) Nomenclature for sugar-binding subsites in glycosyl hydrolases. *Biochem. J. 321*, 557–559.
14. Cartmell, A., Topakas, E., Ducros, V. M., Suits, M. D., Davies, G. J., and Gilbert, H. J. (2008) The *Cellvibrio japonicus* mannanase CjMan26C displays a unique exo-mode of action that is conferred by subtle changes to the distal region of the active site. *J. Biol. Chem. 283*, 34403–34413.
15. Ducros, V. M., Zechel, D. L., Murshudov, G. N., Gilbert, H. J., Szabo, L., Stoll, D., Withers, S. G., and Davies, G. J. (2002) Substrate distortion by a β-mannanase: Snapshots of the Michaelis and covalent-intermediate complexes suggest a $B_{(2,5)}$ conformation for the transition state. *Angew. Chem., Int. Ed. 41*, 2824–2827.
16. Tailford, L. E., Offen, W. A., Smith, N. L., Dumon, C., Morland, C., Gratien, J., Heck, M. P., Stick, R. V., Bleriot, Y., Vasella, A., Gilbert, H. J., and Davies, G. J. (2008) Structural and biochemical evidence for a boat-like transition state in β-mannosidases. *Nat. Chem. Biol. 4*, 306–312.
17. Offen, W. A., Zechel, D. L., Withers, S. G., Gilbert, H. J., and Davies, G. J. (2009) Structure of the Michaelis complex of β-mannosidase, Man2A, provides insight into the conformational itinerary of mannoside hydrolysis. *Chem. Commun.* (in press).
18. Ionescu, A. R., Whitfield, D. M., Zgierski, M. Z., and Nukada, T. (2006) Investigations into the role of oxacarbenium ions in glycosylation reactions by ab initio molecular dynamics. *Carbohydr. Res. 341*, 2912–2920.
19. Nerinckx, W., Desmet, T., and Claeyssens, M. (2006) *ARKIVOC 13*, 90–116.
20. Pell, G., Szabo, L., Charnock, S. J., Xie, H., Gloster, T. M., Davies, G. J., and Gilbert, H. J. (2004) Structural and biochemical analysis of *Cellvibrio japonicus* xylanase 10C: How variation in substrate-binding cleft influences the catalytic profile of family GH-10 xylanases. *J. Biol. Chem. 279*, 11777–11788.
21. Hogg, D., Woo, E. J., Bolam, D. N., McKie, V. A., Gilbert, H. J., and Pickersgill, R. W. (2001) Crystal structure of mannanase 26A from *Pseudomonas cellulosa* and analysis of residues involved in substrate binding. *J. Biol. Chem. 276*, 31186–31192.
22. Charnock, S. J., Spurway, T. D., Xie, H., Beylot, M. H., Virden, R., Warren, R. A., Hazlewood, G. P., and Gilbert, H. J. (1998) The topology of the substrate binding clefts of glycosyl hydrolase family 10 xylanases are not conserved. *J. Biol. Chem. 273*, 32187–32199.
23. Otwinowski, Z., and Minor, W. (1997) Processing of X-ray diffraction data collected in oscillation mode. *Methods Enzymol. 276*, 307–326.
24. Collaborative Computational Project Number 4 (1994) The CCP4 suite: Programs for protein crystallography. *Acta Crystallogr. D50*, 760–763.
25. Murshudov, G. N., Vagin, A. A., and Dodson, E. J. (1997) Refinement of macromolecular structures by the maximum likelihood method. *Acta Crystallogr. D53*, 240–255.
26. Emsley, P., and Cowtan, K. (2004) Coot: Model-building tools for molecular graphics. *Acta Crystallogr. D60*, 2126–2132.
27. Charnock, S. J., Lakey, J. H., Virden, R., Hughes, N., Sinnott, M. L., Hazlewood, G. P., Pickersgill, R., and Gilbert, H. J. (1997) Key residues in subsite F play a critical role in the activity of *Pseudomonas fluorescens* subspecies *cellulosa* xylanase A against xylooligosaccharides but not against highly polymeric substrates such as xylan. *J. Biol. Chem. 272*, 2942–2951.
28. Koivula, A., Kinnari, T., Harjunpaa, V., Ruohonen, L., Teleman, A., Drakenberg, T., Rouvinen, J., Jones, T. A., and Teeri, T. T. (1998) Tryptophan 272: An essential determinant of crystalline cellulose degradation by *Trichoderma reesei* cellobiohydrolase Cel6A. *FEBS Lett. 429*, 341–346.
29. Mori, H., Bak-Jensen, K. S., Gottschalk, T. E., Motawia, M. S., Damager, I., Moller, B. L., and Svensson, B. (2001) Modulation of activity and substrate binding modes by mutation of single and double subsites $+1/+2$ and $-5/-6$ of barley α-amylase 1. *Eur. J. Biochem. 268*, 6545–6558.
30. Mori, H., Bak-Jensen, K. S., and Svensson, B. (2002) Barley α-amylase Met53 situated at the high-affinity subsite -2 belongs to a substrate binding motif in the $\beta \rightarrow \alpha$ loop 2 of the catalytic $(\beta/\alpha)_8$-barrel and is critical for activity and substrate specificity. *Eur. J. Biochem. 269*, 5377–5390.
31. Jenkins, J., Lo Leggio, L., Harris, G., and Pickersgill, R. (1995) β-Glucosidase, β-galactosidase, family A cellulases, family F xylanases and two barley glycanases form a superfamily of enzymes with 8-fold β/α architecture and with two conserved glutamates near the carboxy-terminal ends of β-strands four and seven. *FEBS Lett. 362*, 281–285.
32. Le Nours, J., Anderson, L., Stoll, D., Stalbrand, H., and Lo Leggio, L. (2005) The structure and characterization of a modular endo-β-1,4-mannanase from *Cellulomonas fimi*. *Biochemistry 44*, 12700–12708.
33. Akita, M., Takeda, N., Hirasawa, K., Sakai, H., Kawamoto, M., Yamamoto, M., Grant, W. D., Hatada, Y., Ito, S., and Horikoshi, K. (2004) Crystallization and preliminary X-ray study of alkaline mannanase from an alkaliphilic *Bacillus* isolate. *Acta Crystallogr. D60*, 1490–1492.
34. Hilge, M., Gloor, S. M., Rypniewski, W., Sauer, O., Heightman, T. D., Zimmermann, W., Winterhalter, K., and Piontek, K. (1998) High-resolution native and complex structures of thermostable β-mannanase from *Thermomonospora fusca*: Substrate specificity in glycosyl hydrolase family 5. *Structure 6*, 1433–1444.
35. Larsson, A. M., Anderson, L., Xu, B., Munoz, I. G., Uson, I., Janson, J. C., Stalbrand, H., and Stahlberg, J. (2006) Three-dimensional crystal structure and enzymic characterization of β-mannanase Man5A from blue mussel *Mytilus edulis*. *J. Mol. Biol. 357*, 1500–1510.
36. Bourgault, R., Oakley, A. J., Bewley, J. D., and Wilce, M. C. (2005) Three-dimensional structure of (1,4)-β-D-mannan mannanohydrolase from tomato fruit. *Protein Sci. 14*, 1233–1241.
37. Sabini, E., Schubert, H., Murshudov, G., Wilson, K. S., Siika-Aho, M., and Penttila, M. (2000) The three-dimensional structure of a *Trichoderma reesei* β-mannanase from glycoside hydrolase family 5. *Acta Crystallogr. D56*, 3–13.
38. Davies, G. J., Mackenzie, L., Varrot, A., Dauter, M., Brzozowski, A. M., Schulein, M., and Withers, S. G. (1998) Snapshots along an enzymatic reaction coordinate: Analysis of a retaining β-glycoside hydrolase. *Biochemistry 37*, 11707–11713.
39. Varrot, A., Schulein, M., and Davies, G. J. (2000) Insights into ligand-induced conformational change in Cel5A from *Bacillus agaradhaerens* revealed by a catalytically active crystal form. *J. Mol. Biol. 297*, 819–828.
40. Money, V. A., Smith, N. L., Scaffidi, A., Stick, R. V., Gilbert, H. J., and Davies, G. J. (2006) Substrate distortion by a lichenase highlights the different conformational itineraries harnessed by related glycoside hydrolases. *Angew. Chem., Int. Ed. 45*, 5136–5140.
41. Vincent, F., Gloster, T. M., Macdonald, J., Morland, C., Stick, R. V., Dias, F. M. V., Prates, J. A. M., Fontes, C. M. G. A., Gilbert, H. J., and Davies, G. J. (2004) Common inhibition of both β-glucosidase and β-mannosidase by isofagomine lactam reflects different conformational itineraries for pyranoside hydrolysis. *ChemBioChem 5*, 1596–1599.
42. Stoll, D., Stalbrand, H., and Warren, R. A. (1999) Mannan-degrading enzymes from *Cellulomonas fimi*. *Appl. Environ. Microbiol. 65*, 2598–2605.